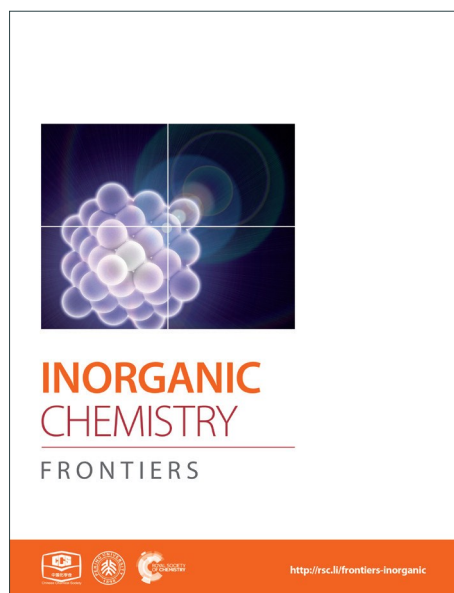
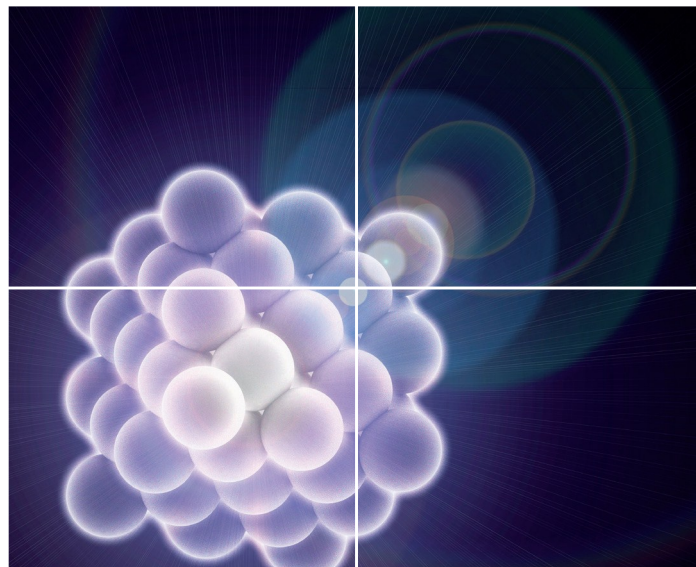


INORGANIC CHEMISTRY

FRONTIERS

Accepted Manuscript



This is an *Accepted Manuscript*, which has been through the Royal Society of Chemistry peer review process and has been accepted for publication.

Accepted Manuscripts are published online shortly after acceptance, before technical editing, formatting and proof reading. Using this free service, authors can make their results available to the community, in citable form, before we publish the edited article. We will replace this *Accepted Manuscript* with the edited and formatted *Advance Article* as soon as it is available.

You can find more information about *Accepted Manuscripts* in the [Information for Authors](#).

Please note that technical editing may introduce minor changes to the text and/or graphics, which may alter content. The journal's standard [Terms & Conditions](#) and the [Ethical guidelines](#) still apply. In no event shall the Royal Society of Chemistry be held responsible for any errors or omissions in this *Accepted Manuscript* or any consequences arising from the use of any information it contains.



Journal Name

ARTICLE

TDDFT studies on chiroptical properties of chiral inorganic polythioanion Möbius strip

Chun-Yan Li, Ting Zhang, Jia-Shu Chi, Li-Kai Yan* and Zhong-Min Su*

Received 00th January 20xx,
Accepted 00th January 20xx

DOI: 10.1039/x0xx00000x

www.rsc.org/

The electronic circular dichroism (ECD) spectra of chiral inorganic polythioanion Möbius strip, $[(\text{Mo}_2\text{S}_2\text{O}_2)_4(\text{OH})_6(\text{C}_4\text{O}_4)(\text{Mo}_2\text{O}_8)]^{4-}$ (**1a**) and its 1e- and 2e-reduced forms were investigated by using the time-dependent density functional theory (TDDFT) method. The simulated UV spectra of **1a** agree well with the experimental spectra, confirming that CAM-B3LYP hybrid functional can well predict the excitation energies of polythioanion. The shapes of ECD bands for reduced forms are similar with that of **1a**, while the rotatory strengths clearly increase with the incoming reduced electrons. The ECD spectra of **1a** are mainly assigned to the charge transfer from $\{\text{C}_4\text{O}_4\}$ unit and S atoms to Mo and terminal oxygen (O_t) atoms. The $\{\text{C}_4\text{O}_4\}$ unit is main chiroptical chromophore. For reduced forms, the charge transfer from S atoms to Mo atoms significant increases with the reduced electrons. It is reasonable to predict that the chiral transfer from $\{\text{C}_4\text{O}_4\}$ unit to $\{\text{Mo}_2\text{S}_2\text{O}_2\}$ unit is generated during the reduced process.

Introduction

Chiral materials have attracted much attention, not only because of their potential applications in enantioselective catalysis, materials science, biology, and medicine, but also due to their intriguing variety of architectures and topologies.^{1,2} Various compounds including organic molecules,³ zeolite⁴ and polyoxoanions⁵ with chiral structures have been reported. In recent years, polyoxoanions of tungsten, molybdenum, and vanadium have been the subject of interest since their wide variety of compositions, structures, and properties gave rise to numerous important applications.⁶ However, thiometalates are less common than oxometalates.⁷ Fortunately, the synthetic approaches for the formation of thiopolyoxometalates (TPOMs) with sulfur-containing cationic building blocks $\{\text{Mo}_2\text{O}_2\text{S}_2\}^{2+}$ and $\{\text{Mo}_3\text{S}_4\}^{4+}$ have been improved.⁸ Cronin and co-workers reported a chiral polythioanion ring cluster $[(\text{Mo}_2\text{S}_2\text{O}_2)_4(\text{OH})_6(\text{C}_4\text{O}_4)(\text{Mo}_2\text{O}_8)]^{4-}$ (**1a**) using $[\text{Mo}_2\text{S}_2\text{O}_2(\text{H}_2\text{O})_6]^{2+}$ and squarate dianion.⁹ At the same time, the nonchiral cluster **1b** can be obtained, which is an isomer of **1a**. Intriguingly, the chiral cluster **1a** was always firstly produced in high yield, and **1b** was crystallized in a much lower yield after **1a** was separated from the mother liquor.⁹ It was noticed that four $\{\text{Mo}_2\text{O}_2\text{S}_2\}$ units in chiral cluster **1a** are connected to each other by hydroxo double bridges, and the ring is incorporated by a $\{\text{Mo}_2\text{O}_8\}$ unit, resulting in the topology of a Möbius strip, which phenomenon does not occur

to **1b**. Except the synthesized strategy and novel structure of chiral cluster **1a**, the further investigation on the related properties is especially attractive.

Chiral compounds or chiroptical properties are usually monitored by circular dichroism (CD) spectroscopy, which refers to the differential absorption of left- and right-circularly polarized light¹⁰ and was first discovered by Cotton and co-workers in 1896.¹¹ Chiral POM-based materials are often characterized by their CD spectra over the ultraviolet-visible (UV-vis) region, which is related to the electronic excitations and called the electronic CD (ECD) spectra. ECD spectra can provide information such as the origin of optical activity and the elucidation of electronic structures, the assignment of transition, and the determination of absolute configuration for chiral molecules.¹²⁻¹⁴ Nowadays, the phenomenon is emerged that the theoretical methods are trusted for understanding chemistry. The theoretical investigations on the electronic and chiroptical properties of chiral compound at the molecular scale would be valuable from both the theoretical and practical points of view. The previous works have already shown that theoretical approaches are very helpful for explaining the ECD spectra of chiral isomers.¹⁵⁻¹⁷ The density functional theory (DFT), because of its accuracy and computational efficiency, has in recent years become a popular approach for studying the optical activity. It has been applied to calculate the ECD spectra of a number of transition-metal complexes¹⁸⁻²⁵ and POMs.²⁶⁻²⁹ In 2012, Zhongmin Su and co-workers reported that the chirality transfer from chiral carbon atom to POM cage increases as the polyanion is reduced through the studies of electronic transition.²⁷ These studies show fair agreement between DFT and experimental ECD spectra.

In the present work, the time-dependent DFT (TD-DFT)

Institute of Functional Material Chemistry, Faculty of Chemistry, Northeast Normal University, Changchun 130024, P. R. China. E-mail: yanlk924@nenu.edu.cn, zmsu@nenu.edu.cn; Fax: +86-0431-85684009

*Electronic Supplementary Information (ESI) available: See DOI: 10.1039/x0xx00000x

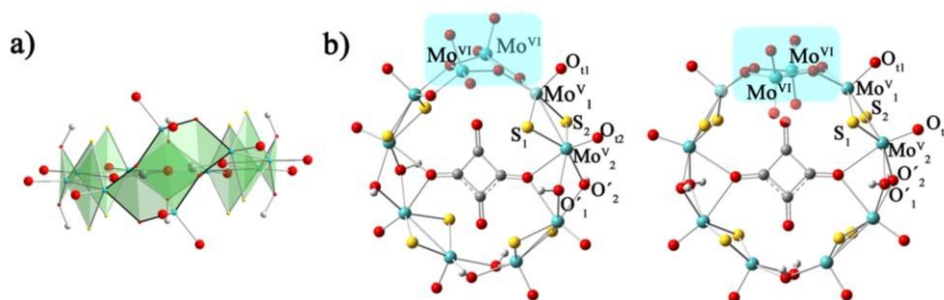


Fig. 1. The optimized structures $[(\text{Mo}^{\text{V}}_2\text{S}_2\text{O}_2)_4(\text{OH})_6(\text{Mo}^{\text{VI}}_2\text{O}_8)(\text{C}_4\text{O}_4)]^{4-}$, (a) side view of **1a**; (b) top view of **1a** (left) and **1b** (right).

method is applied to evaluate the ECD spectra of chiral polythioanion ring cluster $[(\text{Mo}_2\text{S}_2\text{O}_2)_4(\text{OH})_6(\text{C}_4\text{O}_4)(\text{Mo}_2\text{O}_8)]^{4-}$ (**1a**) and its one- and two-electron reduced forms, **[1a]⁻** and **[1a]²⁻**. We concern the following questions: (1) what are the origins of the ECD spectra for **1a** and its reduced forms? (2) which is the chiroptical chromophore? $\{\text{Mo}_2\text{S}_2\text{O}_2\}$, $\{\text{Mo}_2\text{O}_8\}$ or $\{\text{C}_4\text{O}_4\}$? (3) Whether the chirality transfer occurs when **1a** is reduced. Therefore, the ECD spectra of **1a** and its reduced forms were simulated, and the electronic structures and transitions as well as the origins of the ECD spectra were analyzed by using DFT and TD-DFT methods. At the same time, **1b** was also studied for comparison with **1a**.

Computational details

The calculation models are shown in Fig. 1. The geometry optimizations of all studied clusters were performed with the Gaussian 09 package³⁰ at DFT level by means of hybrid exchange-correlation PBE0 functional.^{31,32} Considering the relativistic effects for the transition metal ions, LANL2DZ basis set containing the effective core potential (ECP) proposed by Hay and Wadt³³ was applied for Mo atoms. The 6-31G* basis set³⁴ was used for H, C, O and S atoms. The solvent effect was included during the geometry optimization in solvent water by means of the polarizable continuum model (PCM)³⁵ as implemented in Gaussian09. Geometry optimizations were carried out with symmetry constraints, C_2 and C_{2v} for **1a** and **1b**, respectively.

TDDFT is one of the most popular methods for calculating electron absorption spectra in quantum chemistry owing to the accuracy and efficiency.^{17, 27, 36} Our recent work confirmed that the CAM-B3LYP hybrid functional³⁷ using Coulomb-attenuating method is effective to describe the charge-transfer excitations and absorption properties for giving excitation energies. Therefore, the TDDFT/CAM-B3LYP method and 6-31G*/LanL2DZ (6-31G* for C, H, O, and S atoms; LanL2DZ for Mo atom) were employed to calculate the ECD spectra. The solvent effect was employed by PCM in TDDFT calculations. Gaussian band shape with a bandwidth of 0.22 eV was used to simulate the UV-vis/ECD spectra.

Results and discussion

Geometric and Electronic Structure

From the experiment, the chiral cluster **1a** was always produced first in high yield, and **1b** crystallized in a much lower yield after **1a** was separated from the mother liquor.⁹ **1a** is constructed by $\{\text{Mo}^{\text{V}}_2\text{O}_2\text{S}_2\}$ units, which are connected to each other by hydroxo double bridges, and $\{\text{Mo}^{\text{VI}}_2\text{O}_8\}$ was incorporated. The $[\text{Mo}^{\text{VI}}_2\text{O}_8]^{4-}$ unit adopts two distinct configurations in **1a** and **1b**, which results in the key difference between **1a** and **1b**. Mo^{VI} atoms are five-coordinated in **1a** while the Mo^{VI} atoms in **1b** are four-coordinated. The symmetries for **1a** and **1b** are C_2 and C_{2v} , respectively. The total energies of **1a** and **1b** were calculated by different functionals (PBE0, B3LYP, and BP86) and basis sets (6-31G*, 6-31+G*, 6-31++G*/LanL2DZ). The relative energies that are defined by $\Delta E = E_{1a} - E_{1b}$ are collected in Table S1 (Supporting Information) indicate the energy difference between **1a** and **1b** is small. It suggests that **1a** and **1b** are not thermodynamic controlled, which is in good agreement with experimental phenomenon.⁹ The optimized bond lengths for $[\text{Mo}^{\text{VI}}_2\text{O}_8]^{4-}$ unit in **1a** and **1b** are shown in Table 1, and the experimental X-ray parameters are also included. It can be seen that the experimental structures are well reproduced by the present calculations.

In order to study the electronic properties of **1a** and **1b**, the frontier molecular orbitals (FMOs) are studied and shown in Fig. 2. It is clearly seen that the FMOs for **1a** and **1b** are different. The highest occupied molecular orbital (HOMO) in **1a** mainly delocalizes over $\{\text{C}_4\text{O}_4\}$ unit and the lowest unoccupied molecular orbital (LUMO) localizes on the two $\{\text{Mo}^{\text{V}}_2\text{O}_2\text{S}_2\}$ units, which are away from $\{\text{Mo}^{\text{VI}}_2\text{O}_8\}$ unit. The HOMO of **1b** mainly localizes on $\{\text{Mo}^{\text{VI}}_2\text{O}_8\}$ unit and two $\{\text{Mo}^{\text{V}}_2\text{O}_2\text{S}_2\}$ units, which are adjacent to $\{\text{Mo}^{\text{VI}}_2\text{O}_8\}$, and $\{\text{C}_4\text{O}_4\}$ slightly contributes to HOMO, while the LUMO delocalizes over the $\{\text{Mo}^{\text{VI}}_2\text{O}_8\}$ and $\{\text{Mo}^{\text{V}}_2\text{O}_2\text{S}_2\}$ units. Although the distributions of FMOs for **1a** and **1b** are different, the energy levels of FMOs

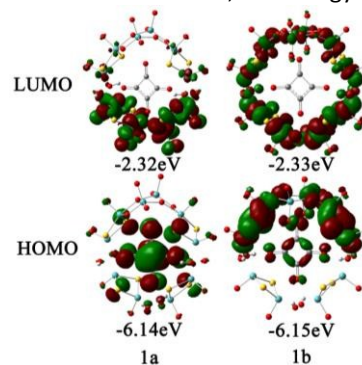


Fig. 2. Frontier molecular orbitals for **1a** and **1b**.

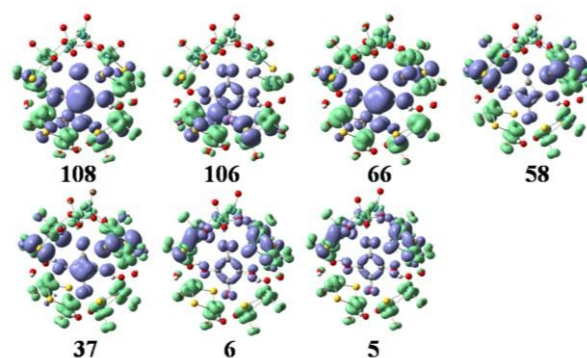
Table 1. Experimental and Theoretical Optimized Bond Lengths for $\{\text{Mo}^{\text{VI}}_2\text{O}_8\}$ unit in **1a** and **1b**

bond length (Å)	1a		1b	
	exp	cal	exp	cal
$\text{Mo}^{\text{V}}_1\text{-Mo}^{\text{V}}_2$	2.841	2.871	2.827	2.859
$\text{Mo}^{\text{V}}_1\text{-O}_{11}$	1.682	1.687	1.681	1.686
$\text{Mo}^{\text{V}}_2\text{-O}_{12}$	1.682	1.689	1.685	1.688
$\text{Mo}^{\text{V}}_2\text{-O}'_1$	2.113	2.136	2.071	2.123
$\text{Mo}^{\text{V}}_2\text{-O}'_2$	2.098	2.115	2.081	2.123
$\text{Mo}^{\text{V}}_1\text{-S}_1$	2.325	2.348	2.304	2.347
$\text{Mo}^{\text{V}}_1\text{-S}_2$	2.301	2.358	2.318	2.347
$\text{Mo}^{\text{V}}_2\text{-S}_1$	2.328	2.340	2.304	2.328
$\text{Mo}^{\text{V}}_2\text{-S}_2$	2.302	2.325	2.307	2.328

are similar. From the LUMO distribution of **1a**, it proposes that the one-electron reduced centre is the $\{\text{Mo}^{\text{V}}_2\text{O}_2\text{S}_2\}$ units, which are away from $\{\text{Mo}^{\text{VI}}_2\text{O}_8\}$ unit.

The ECD Spectra of **1a**

The simulated UV-vis spectra of **1a** are presented in Fig. 3 (left), and the comparison for simulated and experimental spectra are shown in Fig. 3 (inset). The simulated spectra are in good agreement with the experimental one, confirming that the CAM-B3LYP hybrid functional and 6-31G*/LanL2DZ basis set used in this work are appropriate. Compared with the experimental data, the simulated maximum absorption for UV-vis spectra is bathochromically shifted about 0.15 eV. At the same time, we have calculated the UV spectra of **1b**, which is shown in Fig S1. The peaks of **1b** are similar with that of **1a**, while **1b** has another peak in 3.5eV. The main absorption band of **1a** at $\Delta E \approx 4.6$ eV is mainly simulated from some intimate excited states with uniform oscillator strengths, such as states 106 and 108 Fig.3 (left). These excited states are usually composed of many electron transition, therefore an electron density difference map (EDDM) is used to analyze the molecular orbitals involved in the crucial electron transitions, as well as to assign the electron transition origins for the ECD spectrum. The EDDMs were calculated using the Gauss-Sum 2.2.3 software package.³⁸ Electron densities move from the purple area to the green area in this work. The EDDMs for excited states 5, 6, 37, 58, 66, 106 and 108 of **1a** are shown in Fig. 4. The EDDMs show that the UV-vis spectra are mainly

**Fig. 4.** The EDDMs for main excited states which contribute to the UV-vis spectra of **1a**. (Electron densities move from the purple area to the green area)

ascribed to the charge transfer (CT) transitions from the $\{\text{C}_4\text{O}_4\}$ unit and S atoms to Mo atoms. For low-lying UV-vis spectra, CT transitions from S atoms in $\{\text{Mo}^{\text{V}}_2\text{O}_2\text{S}_2\}$ units closed to $\{\text{Mo}^{\text{VI}}_2\text{O}_8\}$ increase in comparison to the high-lying range.

The simulated ECD spectra for **1a** are shown in Fig. 3 (right). The ECD bands were simulated by using a Gaussian band shape with a bandwidth of $\sigma = 0.22$ eV and are indicated by capital letters. From Fig. 3 (right), the simulated ECD spectra of **1a** show six bands: a positive ECD band at $\Delta E \approx 4.68$ eV (band A), a weak negative ECD band at $\Delta E \approx 4.47$ eV (band B), a weak positive ECD band at $\Delta E \approx 4.07$ eV (band C), a negative ECD band at $\Delta E \approx 3.66$ eV (band D), a broad positive ECD band at $\Delta E \approx 3.37$ eV (band E), and a weak negative ECD band at $\Delta E \approx 2.84$ eV (band F). The Cotton effects around $\Delta E = 4.68$ eV (A) \sim 3.66 eV (D) originate from the rotatory absorptions of the excitation at $\Delta E \approx 4.68$ eV in the UV-vis spectra. We found that both the absorption intensity and rotatory strength for states 106, 66 and 37 are larger, which give the main contributions to UV-vis and ECD spectra. It confirms that the shoulders in the absorption spectrum coincide with the CD bands.

For clarity, the calculated excitation energies, transition states, rotatory strengths, and charge-transfer characters for the ECD bands of **1a** are presented in Table 2, and the EDDM is illustrated in Table S2 (Supporting Information). Although the ECD bands A-F of **1a** are from different excited states, the origins of these bands are mainly assigned to CT from O and C atoms of $\{\text{C}_4\text{O}_4\}$ unit and S atoms to Mo and O_t atoms.

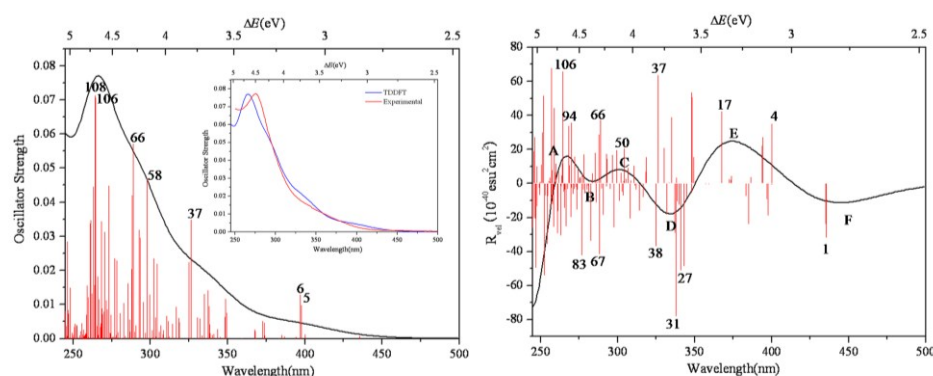
**Fig. 3.** Calculated UV-vis spectra of **1a** (left); Experimental and simulated UV-vis spectra of **1a** (inset); Calculated ECD spectra of **1a** (right). The half bandwidth of $\sigma = 0.22$ eV.

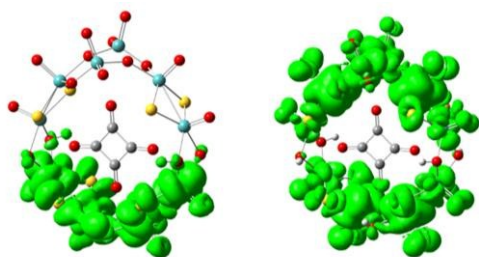
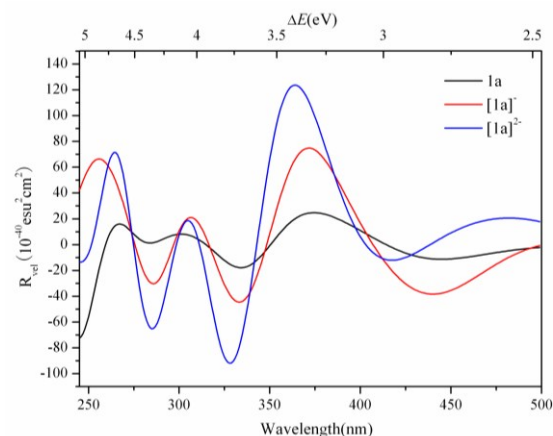
Table 2. Excitation Energies (ΔE , eV), Transition States, Rotatory Strengths, and Charge Transfers for the ECD Bands of **1a**

Band	ΔE (eV)	Transition state (s)	Rotatory strength(s)	Charge transfer
A	4.68	106,94	65.79, 35.62	O and C atoms of squarate anions and S to Mo, O _i
B	4.47	67, 66, 83	-41.55, 37.03, -41.86	O and C atoms of squarate anions and S to Mo, O _i
C	4.07	50	20.40	O and C atoms of squarate anions and S to Mo, O _i
D	3.66	38, 37, 31, 27	-36.58, 63.61, -77.86, -50.79	O and C atoms of squarate anions and S to Mo, O _i
E	3.37	17, 4	42.11, 34.85	O and C atoms of squarate anions and S to Mo, O _i
F	2.84	1	-31.58	O and C atoms of squarate anions and S to Mo, O _i

The ECD Spectra of 1e-/2e-Reduced Cluster of **1a**

In order to check whether the redox process induces the chiral transfer, in other words, the influence of the reduction on the CD spectra, the electronic structures and ECD spectra of 1e-/2e-reduced cluster of **1a** were investigated. Both the closed-shell singlet and the open-shell triplet ground states of the 2e-reduced cluster are considered, and the results show that the total energy of the open-shell cluster is 0.239 eV lower than that of the closed-shell cluster. Thus, the open-shell cluster is more stable than the closed-shell cluster. Therefore, the ECD spectrum of open-shell cluster is further studied. The spin density distributions of **[1a]⁻** and **[1a]²⁻** are presented in Fig. 5. For one electron reduced process, the reduced centers concentrate on four Mo atoms, which are far from {Mo^{VI}O₈} unit. From Table S3 (Supporting Information), the spin density for these four Mo atoms are 0.204, 0.187, 0.187 and 0.204, and the NBO charges are 0.389, 0.379, 0.379 and 0.389, respectively. The spin density, NBO and Mulliken charges for **[1a]²⁻** are collected in Table S4. It is clearly seen that the extra electrons delocalize over eight Mo atoms.

The FMOs of **[1a]⁻** and **[1a]²⁻** are shown in Fig.S2 and S3, which are obviously different with those of **1a**. The α -HOMO and α -LUMO of **[1a]⁻** localize on the two {Mo^VO₂S₂} units, which are away from {Mo^{VI}O₈} unit. The β -HOMO mainly localizes over {C₄O₄} unit, while the β -LUMO mainly localizes over {Mo^{VI}O₈} unit and two {Mo^VO₂S₂} units. The α -HOMO-1 for **[1a]⁻** is similar with the HOMO of **1a**. The α -HOMO and α -LUMO of **[1a]²⁻** localize on {Mo^{VI}O₈} unit and two {Mo^VO₂S₂} units. The β -HOMO of **[1a]²⁻** localizes on {C₄O₄} unit and two {Mo^VO₂S₂} units, which are adjacent to {Mo^{VI}O₈}, and the β -LUMO mainly delocalizes on the two {Mo^VO₂S₂} units, which are away from {Mo^{VI}O₈} unit. The α -HOMO-2 of **[1a]²⁻** is similar with the HOMO of **1a**. From the differences on FMOs between **1a** and its reduced forms, it might lead to the different charge transition of and affect the ECD spectra.

**Fig. 5.** Spin density distribution computed for **[1a]⁻** (left) and **[1a]²⁻** (right).**Fig. 6.** Simulated ECD spectra of **1a**, **[1a]⁻** and **[1a]²⁻**

The ECD spectra of **[1a]⁻** and **[1a]²⁻** were simulated and illustrated in Fig. 6, and the ECD spectra of **1a** are also included for comparison. The ECD bands of 1e-/2e-reduced forms of **1a** are similar to that of **1a**, and the low energy ECD bands are slightly bathochromically shifted with the incoming electrons, while the rotatory strengths significantly increase. The excitation energies, transition states and rotatory strengths for ECD bands of **[1a]⁻** and **[1a]²⁻** are summarized in Table 3 and 4, and EDDMs for crucial transitions contributing to ECD spectra are shown in Fig. S4 and S5 (Supporting Information). For **[1a]⁻**, the EDDMs show that the excited states 122, 152, 156, 188, 196, 327, and 338 are ascribed to the charge transfer from {C₄O₄} unit to Mo atoms, and the excited states 46, 52, 87, 88, 103, 104, and 124 are contributed by the charge transfer from Mo and S atoms in {Mo^VO₂S₂} to Mo and O atoms in {Mo^{VI}O₈}. According to these results, the origins of the chiroptical activity for **[1a]⁻** are assigned to two types charge transfer transitions, one is from to {C₄O₄} unit to {Mo^VO₂S₂} and/or {Mo^{VI}O₈} units, another one is within {Mo^VO₂S₂} and {Mo^{VI}O₈} units. The charge transfer transitions of **[1a]²⁻** are similar with that of **[1a]⁻**, while the contribution from charge transfer within {Mo^VO₂S₂} and {Mo^{VI}O₈} units increase compared one-electron reduced form. In comparison with **1a**, except the charge transfer from the {C₄O₄} unit to {Mo^VO₂S₂} and/or {Mo^{VI}O₈} units, the charge transfer transitions from {Mo^VO₂S₂} to {Mo^{VI}O₈} unit in 1e-/2e-reduced forms increase with the incoming electrons.

Table 3. Excitation Energies (ΔE , eV), Transition States and Rotatory Strengths for the ECD Bands of **[1a]**⁻

Band	ΔE (eV)	Transition state (s)	Rotatory strength(s)
A	4.80	338,327	51.91, 43.88
B	4.26	196,188	-29.45, -44.56
C	4.00	156,152	27.38, -57.91
D	3.78	124, 122, 107,104,103	34.03, -34.55, -55.12, -34.19, 56.24
E	3.40	88, 87	51.83, 58.38
F	2.83	52, 46	-48.01, -32.99

Table 4. Excitation Energies (ΔE , eV), Transition States and Rotatory Strengths for the ECD Bands of **[1a]**²⁻

Band	ΔE (eV)	Transition state (s)	Rotatory strength(s)
A	4.73	349,303	24.49, 23.48
B	4.35	278,219	-27.93, -37.36
C	4.10	201,196	-53.70, 27.22
D	3.78	158,150	-71.71, -67.84
E	3.40	130	69.62
F	2.99	76	-33.68

Conclusions

The UV-vis and ECD spectra of chiral inorganic polythioanion Möbius strip $[(\text{Mo}_2\text{S}_2\text{O}_2)_4(\text{OH})_6(\text{C}_4\text{O}_4)(\text{Mo}_2\text{O}_8)]^{4-}$ (**1a**) are investigated by TDDFT calculations. The CAM-B3LYP/6-31G*(LANL2DZ) proves sufficient to predict the excitation energies of studied cluster. It is interesting to find that the one electron reduced centers concentrate on four Mo atoms, which are far from $\{\text{Mo}^{\text{VI}}_2\text{O}_8\}$ unit. For two electron reduced process, the extra electrons delocalize over eight Mo atoms including six Mo^{V} and two Mo^{VI} atoms. The simulated ECD spectra of **1a** show six bands, which originate from the charge transfer from O and C atoms of $\{\text{C}_4\text{O}_4\}$ unit and S atoms to Mo and O_t atoms. It proposes that $\{\text{C}_4\text{O}_4\}$ unit plays a role as an optically active chromophore and contributor to the absorptions of ECD spectra of **1a**. The shapes for ECD bands of 1e-/2e-reduced forms of **1a** (**[1a]**⁻ and **[1a]**²⁻) are similar to that of **1a**, while the rotatory strengths significantly increase. In comparison with **1a**, except the charge transfer from the $\{\text{C}_4\text{O}_4\}$ unit to $\{\text{Mo}^{\text{V}}_2\text{S}_2\text{O}_2\}$ and/or $\{\text{Mo}^{\text{VI}}_2\text{O}_8\}$ units, the charge transfer transitions from $\{\text{Mo}^{\text{V}}_2\text{O}_2\text{S}_2\}$ to $\{\text{Mo}^{\text{VI}}_2\text{O}_8\}$ unit in 1e-/2e-reduced forms increase with the incoming electrons. The chirality transfer from $\{\text{C}_4\text{O}_4\}$ unit to $\{\text{Mo}^{\text{V}}_2\text{O}_2\text{S}_2\}$ and $\{\text{Mo}^{\text{VI}}_2\text{O}_8\}$ units is obvious with the incoming reduced electrons.

Acknowledgements

The authors gratefully acknowledge financial support by NSFC (21403033, 21203020), the Science and Technology Development Planning of Jilin Province (201201067).

Notes and references

- H. Y. An, E. B. Wang, D. R. Xiao, Y. G. Li, Z. M. Su and L. Xu, *Angew. Chem. Int. Ed.*, 2006, **45**, 904.
- A. Shundo, K. Hori, T. Ikeda, N. Kimizuka and K. Tanaka, *J. Am. Chem. Soc.*, 2013, **135**, 10282.
- E. Deniz, M. Tomasulo, S. Sortino and F. M. Raymo, *J. Phys. Chem. C* 2009, **113**, 8491.
- J. Sivaguru, T. Poon, R. Franz, S. Jockusch, W. Adam and N. J. Turro, *J. Am. Chem. Soc.*, 2004, **126**, 10816.
- F. P. Xiao, J. Hao, J. Zhang, C. L. Lv, P. C. Yin, L. S. Wang and Y. G. Wei, *J. Am. Chem. Soc.*, 2010, **132**, 5956.
- D. L. Long, R. Tsunashima and L. Cronin, *Angew. Chem. Int. Ed.*, 2010, **49**, 1736.
- M. T. Pope and A. Müller, *Angew. Chem.*, 1991, **103**, 56; *Angew. Chem. Int. Ed. Engl.*, 1991, **30**, 34.
- E. Cadot, M.N. Sokolov, V.P. Fedin, C. Simonnet-Jégat, S. Floquet and F. Sécheresse, *Chem. Soc. Rev.*, 2012, **41**, 7335.
- H. Y. Zang, H. N. Miras, J. Yan, D. L. Long and L. Cronin, *J. Am. Chem. Soc.*, 2012, **134**, 11376.
- E. I. Solomon and A. B. P. Lever, *Wiley-Interscience: New York*, 1999.
- A. Cotton, *Ann. Chim. Phys.*, 1896, **8**, 347.
- L. Velluz, A. Legrand and M. Grosjean, *Wiley-VCH: New York*, 1969.
- A. Rodger, *Oxford University Press: Oxford, U.K.*, 1997.
- N. Berova, K. Nakanishi and R. W. Woody, *Wiley-VCH: New York*, 2000.
- D. Y. Du, L. K. Yan, Z. M. Su, S. L. Li, Y. Q. Lan and E. B. Wang, *Coord. Chem. Rev.*, 2013, **257**, 702.
- J. Fan and T. Ziegler, *Chirality* 2011, **23**, 155.
- Y. M. Sang, L. K. Yan, J. P. Wang and Z. M. Su, *J. Phys. Chem. A* 2012, **116**, 4152.
- A. Vargas, M. Zerara, E. Krausz, A. Hauser and L. M. Lawson Daku, *J. Chem. Theor. Comput.*, 2006, **2**, 1342.
- P. W. Thulstrup and E. Larsen, *Dalton Trans.*, 2006, **14**, 1784.
- F. E. Jorge, J. Autschbach and T. Ziegler, *J. Am. Chem. Soc.*, 2005, **127**, 975.
- J. Fan and T. Ziegler, *Inorg. Chem.*, 2008, **47**, 4762.
- F. J. Coughlin, M. S. Westrol, K. D. Oyler, N. Byrne, C. Kraml, E. Zysman-Colman, M. S. Lowry and S. Bernhard, *Inorg. Chem.*, 2008, **47**, 2039.
- F. J. Coughlin, K. D. Oyler, R. A. Pascal, Jr and S. Bernhard, *Inorg. Chem.*, 2008, **47**, 974.
- J. Fan, M. Seth, J. Autschbach and T. Ziegler, *Inorg. Chem.*, 2008, **47**, 11656.
- M. Jawiczuk, M. Górecki, A. Suszczyńska, M. Karchier, J. Jaźwiński and J. Frelek, *Inorg. Chem.*, 2013, **52**, 8250.
- Y. M. Sang, L. K. Yan, N. N. Ma, J. P. Wang and Z. M. Su, *J. Phys. Chem. A* 2013, **117**, 2492.
- J. P. Wang, G. C. Yang, L. K. Yan, W. Guan, S. Z. Wen and Z. M. Su, *Dalton Trans.*, 2012, **41**, 10097.
- J. P. Wang, L. K. Yan, G. C. Yang, W. Guan and Z. M. Su, *J. Mol. Graphics Modell.* 2012, **35**, 49.
- L. K. Yan, X. López, J. J. Carbó, R. Sniatynsky, D. C. Duncan and J. M. Poblet, *J. Am. Chem. Soc.*, 2008, **130**, 8223.
- M. J. Frisch, G. W. Trucks, H. B. Schlegel, G. E. Scuseria, M. A. Robb, J. R. Cheeseman, G. Scalmani, V. Barone, B. Mennucci, G. A. Petersson, H. Nakatsuji, M. Caricato, X. Li, H. P. Hratchian, A. F. Izmaylov, J. Bloino, G. Zheng, J. L. Sonnenberg, M. Hada, M. Ehara, K. Toyota, R. Fukuda, J. Hasegawa, M. Ishida, T. Nakajima, Y. Honda, O. Kitao, H. Nakai, T. Vreven, J.A. Montgomery Jr., J. E. Peralta, F. Ogliaro, M. Bearpark, J. J. Heyd, E. Brothers, K. N. Kudin, V. N. Staroverov, R. Kobayashi, J. Normand, K. Raghavachari, A. Rendell, J.C. Burant, S. S. Iyengar, J. Tomasi, M. Cossi, N. Rega, J. M. Millam, M. Klene, J. E. Knox, J. B. Cross, V. Bakken, C. Adamo, J. Jaramillo, R. Gomperts, R. E. Stratmann,

ARTICLE

Journal Name

- O. Yazyev, A. J. Austin, R. Cammi, C. Pomelli, J. W. Ochterski, R. L. Martin, K. Morokuma, V. G. Zakrzewski, G. A. Voth, P. Salvador, J. J. Dannenberg, S. Dapprich, A. D. Daniels, O. Farkas, J. B. Foresman, J. V. Ortiz, J. Cioslowski, D. J. Fox, Gaussian 09, Revision D.01, Gaussian, Inc., Wallingford, CT, 2009.
- 31 J. P. Perdew, K. Burke and M. Ernzerhof, *Phys. Rev. Lett.*, 1996, **77**, 3865.
- 32 J. P. Perdew, K. Burke and M. Ernzerhof, *Phys. Rev. Lett.*, 1997, **78**, 1396.
- 33 P. J. Hay and W. R. Wadt, *J. Chem. Phys.*, 1985, **82**, 270.
- 34 (a) M. M. Francl, W. J. Pietro, W. J. Hehre, J. S. Binkley, M. S. Gordon, D. J. Defrees and J. A. Pople, *J. Chem. Phys.*, 1982, **77**, 3654. (b) W. J. Hehre, R. Ditchfield and J. A. Pople, *J. Chem. Phys.*, 1972, **56**, 2257. (c) P. C. Hariharan and J. A. Pople, *Theor. Chim. Acta*, 1973, **28**, 213.
- 35 J. Tomasi, B. Mennucci and R. Cammi, *Chem. Rev.*, 2005, **105**, 2999.
- 36 B. Hasenknopf, K. Micoine, E. Lacote, S. Thorimbert, M. Malacria and R. Thouvenot, *Eur. J. Inorg. Chem.*, 2008, **32**, 5001.
- 37 T. Yanai, D. Tew and N. Handy, *Chem. Phys. Lett.*, 2004, **393**, 51.
- 38 N. M. O'boyle, A. L. Tenderholt and K. M. Langner, *J. Comput. Chem.*, 2008, **29**, 839.